ANNUAL REVIEWS

Annual Review of Biophysics

Free Energy Methods for the Description of Molecular Processes

Christophe Chipot[1,2,3,4]

[1]Laboratoire International Associé Centre National de la Recherche Scientifique and University of Illinois at Urbana-Champaign, Unité Mixte de Recherche n°7019, Université de Lorraine, Vandœuvre-lès-Nancy, France; email: chipot@illinois.edu

[2]Theoretical and Computational Biophysics Group, Beckman Institute, University of Illinois at Urbana-Champaign, Urbana, Illinois, USA

[3]Department of Physics, University of Illinois at Urbana-Champaign, Urbana, Illinois, USA

[4]Department of Biochemistry and Molecular Biology, The University of Chicago, Chicago, Illinois, USA

Annu. Rev. Biophys. 2023. 52:113–38

First published as a Review in Advance on January 10, 2023

The *Annual Review of Biophysics* is online at biophys.annualreviews.org

https://doi.org/10.1146/annurev-biophys-062722-093258

Keywords

free energy, computer simulations, importance sampling, enhanced sampling, recognition and association, permeation, conformational transitions

Abstract

Efforts to combine theory and experiment to advance our knowledge of molecular processes relevant to biophysics have been considerably enhanced by the contribution of statistical-mechanics simulations. Key to the understanding of such molecular processes is the underlying free-energy change. Being able to accurately predict this change from first principles represents an appealing prospect. Over the past decades, the synergy between steadily growing computational resources and unrelenting methodological developments has brought free-energy calculations into the arsenal of tools commonly utilized to tackle important questions that experiment alone has left unresolved. The continued emergence of new options to determine free energies has also bred confusion amid the community of users, who may find it difficult to choose the best-suited algorithm to address the problem at hand. In an attempt to clarify the current landscape, this review recounts how the field has been shaped and how the broad gamut of methods available today is rooted in a few foundational principles laid down many years ago.

Three examples of molecular processes central to biophysics illustrate where free-energy calculations stand and what are the conceptual and practical obstacles that we must overcome to increase their predictive power.

Contents

1. INTRODUCTION

Complete understanding of molecular processes often requires a close examination of the behavior of their associated free energies. Owing to their ubiquity in the cell machinery, many of these processes have important ramifications in various aspects of biophysics, but also in rational drug design. For this reason, predicting their feasibility by means of theoretical tools is eminently desirable. Over the past decades, considerable progress has been made in the determination of free energies by employing numerical simulations, based on the fundamental principles of statistical mechanics. Although these advances can be ascribed in part to the rapid growth of commonly accessible computational resources, most notably the emergence of fast and inexpensive graphics processing units (GPUs), progress has been facilitated first and foremost by the development of a gamut of methods that have increased the level of efficiency and reliability of free-energy calculations. This progress, however, has come at a price. Navigating through the maze of methods available has become increasingly difficult—especially for the novice practitioner—and so has grasping the conceptual relationships between these methods, the confines of their applicability, and both their suitability and computational efficiency for a given practical problem. The objective of this review is not to provide a superficial account of the behemoth body of work published in recent years, but instead to recapitulate the milestoning main developments that have shaped the field of free-energy calculations. Rather than focusing on their theoretical underpinnings, this review aims to guide the choice of the most relevant method to tackle each problem, most notably for the description of molecular processes. Tracing the roots of the many algorithms available in academic and nonacademic simulation packages—as well as understanding how the methods

that they lean upon are related—is crucial to achieving this goal. After recapping in Section 2 the ontological concepts of free-energy calculations, most prominently the idea of a rare event, which have driven their development, the different families of methods will be presented in an arbitrary classification that, nonetheless, accounts for their common ancestors. I then discuss how the methodology can be used to describe three molecular processes—host–guest recognition and association, permeation, and conformational transitions—showcasing the frontiers reached in this research area. The review closes by outlining the remaining theoretical and practical obstacles, as well as the novel directions being explored to overcome them.

2. BACKGROUND

Why do we turn to free-energy calculations? Since the seminal simulation of Alder & Wainwright (5) in 1957, molecular dynamics (MD) (64) has been employed to investigate chemical objects of increasing complexity (1, 59, 147, 162, 176). A giant step made 20 years later, the simulation of the bovine pancreatic trypsin inhibitor using a simple potential energy function, paved the way for the investigation of the intricate machinery of the cell in numerical experiments (129). With the prospect of tackling complex molecular processes by means of computer simulations came also the realization that capturing rare events would require more than unbiased, brute-force simulations. In this case, the notion of a rare event ought to be understood from a numerical perspective, given that the timescales spanned by the molecular processes at hand, as observed macroscopically, largely exceed those amenable to MD. In spite of the extraordinary dilation of time- and size scales made possible in recent years by the deployment of high-performance computing, the yawning gap between these timescales still constitutes a significant obstacle that has hitherto hampered more theoretical discoveries of biophysical relevance.

2.1. Rare Events and Quasinonergodicity

To fully grasp the concept of a rare event from the standpoint of computer simulations, I invoke the ergodic hypothesis, which stipulates that the time averages of some macroscopic variables coincide with their ensemble averages. Said differently, I assume for the molecular processes that I consider that, in the limit of infinite sampling, all possible microstates compatible with the conservation laws are accessible to the chemical objects of interest. Unfortunately, owing to the finite length of computer simulations, a molecular process that is assumed to be ergodic may appear somewhat nonergodic as a result of incomplete sampling of phase space. Under these premises, the outcome of the simulation—most notably the statistical averages—reflects a pronounced dependence on the initial conditions. This shortcoming, which stems from the slow diffusion of the molecular processes at play and the insufficient volume of phase space sampled to guarantee reliable statistical averages, is referred to as quasinonergodicity. In many molecular processes relevant to biophysics, quasinonergodicity arises from high free-energy barriers separating distinct volumes of phase space; these barriers are often insuperable over finite computer simulations or crossed so rarely that the estimated statistical averages are, for all intents and purposes, physically meaningless. Transitions between these volumes of phase space may, therefore, be seen as rare events that are unlikely to occur over the timescales amenable to brute-force MD. Interestingly enough, the same regions of phase space may be connected by narrow, low-energy corridors, but such entropy bottlenecks are equally rarely sampled and, thus, also contribute to quasinonergodicity. At the microscopic level, the significant time span of the molecular processes of interest—making them rare events from a computational standpoint—is rooted in very slow, often entangled degrees of freedom (DOFs) in the chemical objects at play. Thorough sampling of the inherently multidimensional free-energy landscape, encumbered by

large barriers, therefore requires exploration of alternate avenues apart from brute-force MD. Free-energy calculations (34, 120) have emerged as an essential tool to achieve this goal and are metaphorically viewed as computational tweezers that act surgically on the relevant DOFs, along which sampling is performed in a preferential fashion. At this juncture, it is interesting to note that turning to such strategies, referred to as importance sampling, is aimed not just at improving the statistical-average estimates introduced above, but also, perhaps first and foremost, at probing phenomena otherwise inaccessible to brute-force MD, even on specialized computers (163, 173). In a nutshell, the objective is to tackle, in realistic biological objects, molecular processes that span the typical μs-to-s biological timescales without the explicit need of μs-to-s-long computer simulations. In the next section, I discuss how achieving this objective is feasible in practice.

2.2. Progress Variable, Reaction Coordinate, and Transition Pathway

The theory that underlies free-energy calculations was developed a long time ago. Considering, however, the computational limitations when the methodology was originally introduced, numerical applications at that time are understandably scarce (130). In many respects, the foundations for what would become standard methods for the determination of free-energy differences were laid by Kirkwood (111). These methods, which were developed from either perturbation theory or thermodynamic integration (TI), have one common denominator, namely, the notion of order parameter. In his derivation of integral equations for liquid state theory, Kirkwood reconciled statistical mechanics and the concept of degree of evolution introduced by De Donder (49) for chemical reactions. The notion of order—or generalized-extent—parameter was employed to describe progress in the transition between two suitably characterized thermodynamic states, or volumes of phase space separated by a free-energy barrier, and help determine the free-energy difference between them.

To a large extent, the idea of order parameter, which I denote $\xi(\mathbf{x})$, is akin to that of reaction coordinate (RC), which is best described as an application defined on the configurational space, indexing the transformation of interest. Said differently, it is a high-dimensional mathematical construct that measures the transition of the chemical object of interest in configurational space. In practice, under the assumption of timescale separation, $\xi(\mathbf{x})$ is modeled as a low-dimensional subset of collective variables (CVs; also known as course variables), presumed to capture all of the slow DOFs of the molecular process at hand. As a corollary, it is expected that the DOFs not specifically embraced by the subset of CVs are fast ones. Much of the success of importance-sampling simulations (34, 120), therefore, rests upon our intuition in identifying the relevant DOFs and ability to build a suitable low-dimensional CV space. Failure to model the RC in complex chemical objects and, thus, erroneous description of the underlying dynamics generally stem from an overly reductionist view of the CV space. Even if we are not interested in the dynamics of the molecular process, an ill-advised choice of CVs is not innocuous and may result in extremely poor convergence of the free-energy calculation. In other words, although free energy is, indeed, a state function, the determination of which does not depend on the path chosen—and, by construction, in what CV space this path has been established—leaving out important slow DOFs in the CV space may have critical consequences for the efficiency of the computation.

A variety of methods have been devised to identify the relevant CVs associated with transitions in configurational space (3, 13, 28, 30, 146, 149, 177, 190). However, several of these approaches require very long and, thus, costly MD simulations to infer meaningful information. Such is the case for simulations utilized in Markov state models (21, 36). The applicability of these approaches has generally remained limited to small molecular objects, notwithstanding spectacular undertakings marshaling considerable resources only available in the context of distributed computing

(205). A useful concept associated with transition-path theory (18, 195) that can be used to probe the relevance of the chosen CV subspace is the committor (19, 141), i.e., the commitment probability that a trajectory spawned from a given initial condition will reach target state B before crossing reference state A. In the vicinity of states A and B, which are metastabilities of the free-energy landscape, the committor approaches 0 and 1, respectively. The transition region is foliated into isocommittor surfaces crossed by reactive trajectories. The most probable transition pathway (MPTP) connects state A to state B through the mean values of the corresponding transition flux densities (194), and an optimal CV would have a committor of 1/2 at the transition state.

3. CALCULATING THE FREE ENERGY

In a very broad sense, free-energy calculations of molecular processes can be dichotomized in terms of geometrical and alchemical transformations in configurational space (31, 34, 45). Whereas alchemical transformations lean on the malleability of the potential energy function to navigate between two distinct chemical states, geometrical transformations act directly on the spatial coordinates to modify the positional, orientational, and conformational states of the chemical objects at play. Traditionally, alchemical transformations have often been associated with either free-energy perturbation (FEP) (208) or TI (111) calculations, whereby the reference state is progressively alchemized into the target one by altering the potential energy function or specific terms thereof (71, 107). Democratization of free-energy calculations in recent years has been accompanied by the development of legions of algorithms that have contributed to improving both the computational efficiency and the reliability of the methodology but, at the same time, breed confusion amid the community of users. While the tools commonly employed to perform alchemical transformations have remained limited and overall unchanged, barring enhancements to augment their accuracy (4, 35, 37, 100, 102, 108, 164, 165), the same cannot be said for geometrical transformations (27, 47, 48, 67–69, 87, 88, 97, 99, 115, 122, 138, 142, 144, 159, 198, 203, 204), for which seemingly similar approaches can lead to drastically different results. In a broad sense, geometrical transformations can be carried out by means of a variety of approaches that can be categorized into four classes (see **Figure 1**) based on (*a*) probability distributions and histograms, (*b*) perturbation theory, (*c*) nonequilibrium work realizations, and (*d*) gradient-based methods. Owing to the resemblance of some of the numerical schemes belonging to these different categories to their conceptual common denominators, and to the possibility of interweaving them, this categorization is somewhat arguable and, thus, not unique.

3.1. Probability Distributions and Histograms

In the late 1960s, several innovative strategies emerged to palliate the shortcomings of Boltzmann sampling when determining the free-energy difference between two distinct states of configurational space. One of the most influential ideas—the conceptual groundwork for several free-energy methods—is the energy-distribution formalism. In this formalism, the free-energy difference is represented in terms of a one-dimensional integral over the distribution of potential-energy differences between the two states, weighted by either the unbiased or the biased Boltzmann factor (130). Relying on the introduction of a progress variable, Valleau & Card (182) proposed to build a chain of configurational energies bridging the reference and the target states. Multistage sampling, in essence, stratifies the reaction pathway to split the total free-energy change into a sum of free-energy differences between intermediate states, the low-energy regions of which overlap much better than those of the end states. Fifty years later, stratification remains commonly employed as a variance-reduction strategy (120). Closely related to stratification is the problem of finding the optimum free-energy difference between two canonical ensembles on the same configurational

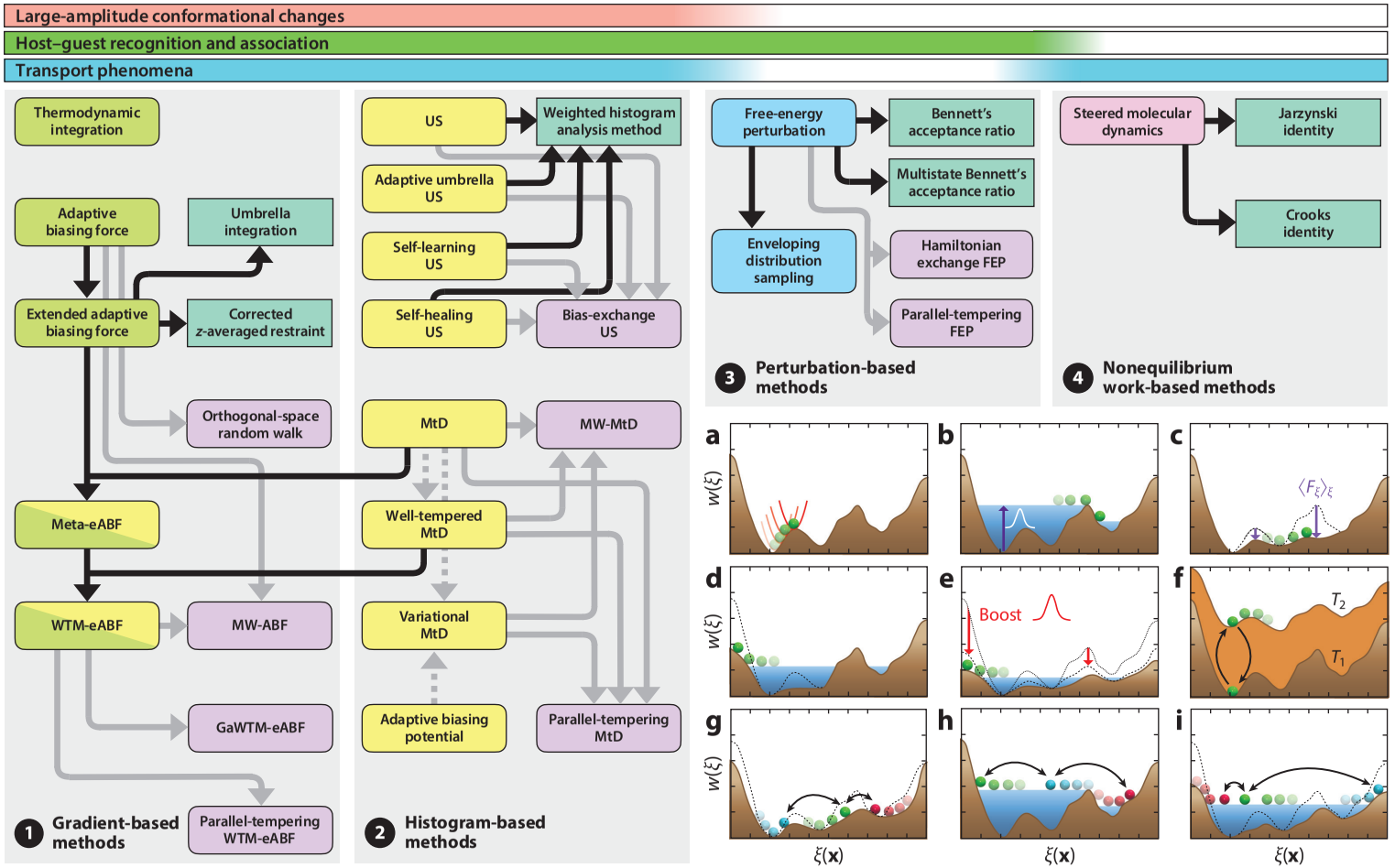

Figure 1

The four classes of free-energy calculations and how they can help address three important molecular processes. Algorithms are shown in colored rounded boxes on the left of each panel, estimators are shown in turquoise squared boxes, and enhanced-sampling schemes are shown in purple rounded boxes. Examples of algorithms and combinations thereof are highlighted in the lower right part of the figure: (*a*) umbrella sampling (US), (*b*) metadynamics (MtD), (*c*) adaptive biasing force (ABF), (*d*) metadynamics-extended ABF (meta-eABF), (*e*) Gaussian-accelerated well-tempered meta-eABF (GaWTM-eABF), (*f*) parallel-tempering, (*g*) multiple-walker ABF (MW-ABF), (*h*) multiple-walker MtD (MW-MtD), and multiple-walker meta-eABF (MW-meta-eABF). Walkers are shown as colored beads evolving on the free-energy landscape. It is noteworthy that, in GaWTM-eABF, the boost term affects the entire potential energy surface.

space, which Bennett (15) addressed by developing the acceptance ratio estimator corresponding to the minimum statistical variance. It is noteworthy that the so-called Bennett acceptance ratio (BAR), which predates the routine use of simulations aimed at predicting free-energy differences, has been broadly employed in bidirectional FEP calculations (150) as a more accurate estimator. The popularity of BAR is due to its ability to supply reasonable estimates of the free-energy difference, even if the overlap between the ensembles is suboptimal. The method has been generalized in a multistate form [multistate BAR (MBAR)] harnessing the statistical data accrued in all intermediate states (164), reducing to BAR in the limit of two distinct states. A related idea to improve the reliability of free-energy estimates consists of sampling the reference ensemble in a sufficiently broad fashion to collect enough data from the low-energy regions of the target ensemble. This central idea constitutes the foundation of umbrella sampling (US) (178), which introduces a non-Boltzmann weighting function into the simulation and subsequently removes it to supply the unbiased probability distribution, from which the free energy is inferred. One of the difficulties raised by US is the design of biases that effectively improve sampling uniformity. The difficulty of guessing these biases, especially for qualitatively new geometrical transformations, explains why the name US and the concept of stratification are often conflated. Probably because they are most efficient when combined, the distinction between them has been lost (160) to the extent that, nowadays, US is generally construed as an approach wherein the reaction pathway is divided into a large number of mutually overlapping regions, and wherein sampling is confined by means of harmonic potentials and sufficiently narrow to obviate the need of an umbrella potential to ensure sampling uniformity. The complete probability distribution along $\xi(\mathbf{x})$ and, thus, the free energy are commonly recovered in an iterative and statistically optimal fashion using tools like the weighted histogram analysis method (WHAM) (114). It is worth noting the connection between WHAM and MBAR, the latter being a zero-width-bin version of the former. Still, US has shortcomings that are often difficult to diagnose, prompting the development of several improvements such as modifying the biases adaptively (11), learning the topology of the free-energy landscape (198), or introducing nonequilibrium (128).

3.2. Perturbation Theory

Nearly 20 years after the trailblazing work of Kirkwood (111), Zwanzig (208) followed a perturbative route to free-energy calculations, demonstrating how the physical properties of a molecule may change upon addition of a rudimentary form of an attractive potential. The high-temperature expansions established by Zwanzig for simple, nonpolar gases form the theoretical ground of the widely popular FEP approach, commonly utilized for the determination of free-energy differences (31, 34, 112). It is noteworthy that the significance of FEP was appreciated much earlier. In fact, Landau (116) included a simple derivation of the perturbation equation in the first edition of his popular textbook on statistical mechanics. Widom (197) established the potential distribution theorem, which is closely related to FEP and can be employed to estimate excess chemical potentials from random insertions of a test particle (196). To a large extent, particle insertion can be seen as a special case of perturbation theory. Practical application of FEP had to wait, however, for the advent of computer architectures endowed with sufficient power to tackle realistic and chemically relevant assemblies of molecules. Although several conceptual ideas for the determination of free-energy differences can be found in earlier, seminal contributions (152, 174, 191), the first concrete application of free-energy calculations is due to Jorgensen & Ravimohan (107), who chose the perturbative route to estimate the relative solvation free energy of methanol and ethane. Toward this end, they devised an elegant paradigm whereby a common topology is shared by the reference and the target states of the transformation. Following a similar strategy, Jorgensen (105) pioneered the estimation of pK_as of simple organic solute in aqueous environments. It is instructive that, barring

remarkable examples (12), these pioneering efforts overall elicited at first only moderate enthusiasm, even though they are viewed today as the turning point for free-energy calculations, paving the way for many challenging applications and advancements that brought the methodology to the status of being predictive. In stark contrast with other classes of methods, most notably those that rely on the estimation of the gradient of the free energy, FEP benefited from far fewer developments, focusing primarily on alternatives to the exponential estimator (15, 164) or the possibility of encapsulating several target states in a single simulation by finding the most suitable reference state (37). Assuming a force field of appropriate accuracy, FEP calculations have proven in recent years capable of supplying the expected answer for a variety of problems (44, 45, 85, 108).

3.3. Nonequilibrium Work Realizations

Another avenue for the exploration of rare events spanning timescales not amenable to MD consists of driving the molecular process out of equilibrium. In a nutshell, steered MD (SMD) (98), also known as force-probe MD (81), rests on the application of an external force along an arbitrary direction of Cartesian space, which results in drifting. In contrast with free-energy calculations carried out at thermodynamic equilibrium, SMD utilizes either a constant or a time-varying force, responsible for marked deviations from equilibrium conditions. Constant-velocity SMD mimics the action of a mobile cantilever akin to that acting on a substrate in atomic-force microscopy (AFM). In practice, a subset of atoms is tethered harmonically to a point moved at constant velocity along an arbitrary direction, which can be viewed as a surrogate RC model. Until recently (7), the timescales spanned by constant-velocity SMD were approximately 10^3–10^6 times shorter than those common in AFM. In other words, to cover reasonable stretches of the reaction pathway, SMD must resort to high pulling speeds, e.g., 10^3 m/s, generating a significant amount of irreversible work, often difficult to relate to equilibrium properties. Yet with the groundbreaking identity established by Jarzynski (99) came the promise of reconciling ensembles of nonequilibrium realizations with the free-energy change underlying a molecular process at equilibrium. A theoretical framework (144) associating SMD simulations with the Jarzynski identity and its maximum-likelihood extension (46, 126) and combining the statistical data accrued in forward and backward pulling realizations showcases the potential of the methodology. Notwithstanding its theoretical appeal, this route to the estimation of free-energy differences raises several concerns. First, the high-pulling regime in constant-velocity realizations is liable to distort the reconstructed free-energy landscape by artificially introducing ruggedness, a phenomenon magnified when pulling of the substrate is significantly faster than the relaxation of its environment. Second, the abundant generation of irreversible work rooted in the high-pulling-speed regime imposes very large numbers of realizations to ensure convergence of the Jarzynski identity. Even with the aid of cumulant expansions (144), acceptable convergence is reached only at the price of performing the pulling experiments in a near-equilibrium regime. The considerable computational effort incurred in these numerous realizations naturally calls into question the impetus to turn to nonequilibrium work experiments when free-energy methods at thermodynamic equilibrium can deliver possibly more reliable results at a much lower cost.

3.4. Gradient-Based Methods

The free energy along the model RC, $\xi(\mathbf{x})$, can be viewed as a potential resulting from the average force that acts in that direction. Said differently, it is the negative of the gradient of this potential, and is thus called the potential of mean force (PMF). In the TI formalism, the average force is the quantity that is determined directly, prior to its integration to supply the free-energy change. The instantaneous force acting along the model RC can be decomposed into an average force

and a random force of zero mean, mirroring the fluctuations of all other DOFs. Seen through a low-dimensional prism, the model RC of the molecular process at hand appears to evolve dynamically in its time-independent PMF, and this evolution is driven by the random force. Under most circumstances, the latter can be safely assumed to be diffusive, thereby rendering a simplified picture of a diffusive process along $\xi(\mathbf{x})$ in the PMF. Amid gradient-based approaches, the adaptive biasing force (ABF) algorithm (39, 48) has emerged as one of the most powerful options for mapping complex free-energy landscapes. In a nutshell, the ABF algorithm adaptively flattens the free-energy landscape by shaving its barriers while preserving the dynamics of the molecular process of interest—in particular, the random fluctuating force. In practice, the instantaneous force exerted along $\xi(\mathbf{x})$ is evaluated at discrete values of it, and its average is updated to supply an estimate of the free-energy gradient. The biasing force, applied once a user-defined number of instantaneous-force samples has been accrued at the different values of $\xi(\mathbf{x})$, cancels exactly the estimated average force. In the long run, this estimate converges toward the average force at equilibrium, yielding a Hamiltonian bereft of an average force acting along $\xi(\mathbf{x})$, reflected in a quasiflat PMF and effectively accelerated dynamics in that direction. In general, convergence to a perfectly flat PMF is seldom achieved, but this requirement is of lesser concern for as long as sampling is sufficiently uniform to allow the shaved barriers to be overcome in response to thermal fluctuations. One of the strengths of the ABF algorithm is that it obviates the need for prior knowledge of the free-energy landscape.

3.5. Enhancing Sampling

Most—if not all—importance-sampling algorithms (34, 120) are vulnerable to barriers in directions orthogonal to the model RC (204), emphasizing again the issues of timescale separation and incompleteness of the CV space, which is missing crucial slow DOFs. In the case of gradient-based algorithms, such as the ABF algorithm, quasinonergodicity is mirrored in its most usual symptoms in an acute sampling nonuniformity, whereby instantaneous-force samples pile up at one end of the reaction pathway. To address the shortcomings that commonly plague ABF simulations, the algorithm, since its original inception, has undergone several improvements, resulting ultimately in more cost-effective free-energy calculations better suited to specific applications (27, 33, 40, 67–69, 87, 133, 170, 203). Most of these improvements lean on the appealing idea that importance-sampling algorithms can be combined seamlessly to augment sampling uniformity. Addition of enhanced-sampling schemes, in the form of boosting potentials (132, 189), multiple copies (133), or temperature exchange (68), has proven useful to explore free-energy landscapes encumbered with high barriers. Resorting to enhanced-sampling techniques (34, 120), in general, and generalized-ensemble schemes (134), in particular, is not limited to the ABF algorithm and its variants—it is also necessary, for instance, in the metadynamics (MtD) (2, 25, 148) and US (101, 168) families of algorithms. In alchemical FEP or TI calculations, in which convergence is burdened by kinetic traps as one chemical species is transformed into an alternate one, sampling can be enhanced by swapping Hamiltonians (200) or by feeding the slowest DOFs, assuming that they can be identified, with boosting potentials (102).

3.6. How Are These Methods Related?

To assess the relative performance of different algorithms, it is often instructive to examine how they are conceptually related. The ABF algorithm is a particular example of a broader family of adaptive algorithms that encompasses the subfamily of adaptive biasing potential (ABP) schemes (120). Notwithstanding their very different roots, local elevation (96), conformational flooding (80), and MtD in its different flavors (10, 115, 183), as well as the Wang-Landau algorithm (187),

are all members of this subfamily, the common trait of which is to penalize regions of configurational space adequately sampled by means of a biasing potential depending on the occupation time at a given value of $\xi(\mathbf{x})$. In the first three of these algorithms, the biasing potential consists of a sum of Gaussian kernels added to the Hamiltonian to flood the valleys of the free-energy landscape, thereby forcing sampling toward marginally visited regions. Because a time-dependent potential is determined—as opposed to its derivative—these three numerical schemes fall into the category of ABP algorithms, which adapt the PMF or the probability distribution along the model RC. In stark contrast, in the ABF subfamily of algorithms, the gradient of the potential is biased. Although one might be tempted to equate the philosophies that underlie these adaptive schemes, there is a fundamental difference between them that is often misconstrued—probability distributions are global properties, whereas gradients are local ones (120). An important consequence of this difference is the necessity to sample over broader ranges of $\xi(\mathbf{x})$ to obtain meaningful probability distributions, which, in turn, may affect adaptation efficiency.

4. HOST–GUEST RECOGNITION AND ASSOCIATION AND STANDARD BINDING AFFINITIES

Host–guest recognition and association is a complex problem of chemistry relevant to a variety of fields. Protein–ligand binding is a very specific example, eminently relevant to biophysics. In this case, the host is the protein, and the guest is the ligand. Reversible association of the binding partners has been the object of a host of theoretical endeavors designed to predict binding affinities within chemical accuracy (20, 22, 24, 50, 51, 55, 56, 73–75, 86, 90, 94, 102, 103, 106, 135, 136, 156, 157, 166, 185, 188, 199, 201). Within the confines of pharmaceutical research, determination of binding free energies from first principles has been an important goal of computer-aided drug design (45), the focus being traditionally more on relative quantities rather than on absolute ones. This strategy can be construed as a way of ranking congeneric lead candidates according to their affinity toward a given target, as opposed to estimating a standard binding free energy. From a practical perspective, this choice is guided by the computational cost incurred in the determination of relative binding affinities between two analogous molecular compounds, which is appreciably lower than that of absolute binding constants (34, 112, 135). In contrast, apparent agreement between relative binding free energies determined from theory and differences between absolute quantities measured experimentally could well be fortuitous and conceal providential cancellation of errors, rendering the diagnostic of potential discrepancies with experiment an arduous task. Assuming a hypothetically perfect force field, the ultimate test of sampling efficacy is the computation of an absolute quantity, e.g., solvation or binding—and, likewise, assuming a hypothetically infinitely long simulation, the ultimate test of the force field would be the same absolute quantity.

Accurate determination of an absolute binding affinity is a complex theoretical problem and a daunting computational challenge even for a small ligand binding to a protein, let alone for two large proteins assembling into a complex. This challenge is deeply rooted in the difficulty of capturing the substantial change in configurational enthalpy and entropy associated with the conformational, orientational, and positional movements of the guest with respect to the host in the course of their reversible binding. Furthermore, in general, little is known about the association pathway. Whereas the bound and unbound states of the partners are well established, knowledge of the path that connects them is at best fragmentary. With the aid of fast, possibly specialized computer architectures, considerably longer atomistic simulations, capable of rendering a chronology of association, can be performed. Restricted to protein–ligand binding, these brute-force simulations capture the molecular process at hand, from the ligand lying away from the protein to its stable docking at the binding site of the protein (24). However informative they are, these

simulations remain restricted to weak binders and only reflect a series of isolated events (58) from which it is difficult to infer meaningful robust thermodynamic quantities, let alone kinetic ones.

One strategy that has proven particularly reliable for the estimation of binding affinities is combining MD and importance-sampling schemes to ensure the adequate exploration of the relevant DOFs. For many years, perturbation theory has been the mainstream approach to tackle protein–ligand association numerically, with the assumption of small enough substrates—thus, precluding the extension of this theory to protein–protein association. Given these premises, the ligand is decoupled reversibly from its aqueous environment, in the unbound state, and in the protein, in the bound state, through scaling of the relevant nonbonded interactions (34, 78, 90, 112). This so-called alchemical route raises, however, several salient issues, chief among which is the violation of thermodynamic microreversibility of the transformation. As the ligand is progressively decoupled from the protein environment (105), it becomes free to wander away from the binding site, resulting in an ill-defined target state and a poor candidate for the reverse, coupling transformation. Owing to the finite length of the simulation, the ambivalent definition of the standard state is magnified by the correlation between it and the size of the cell containing the protein–ligand complex in its aqueous environment (70). This critical shortcoming can be addressed by introducing a series of geometrical restraints to control the movements of the substrate relative to the protein as it is progressively decoupled (89, 90) while improving the sampling efficiency and accelerating convergence of the simulations (184). In a nutshell, a harmonic potential is enforced at one end state of the transformation, to tether the decoupled substrate to the binding site, and is removed at the other end state (20, 78, 161). Enforcement of geometrical restraints on a selection of DOFs is, however, tantamount to a loss of configurational entropy contributing to the binding free energy, which should be accounted for in independent simulations (50, 51, 55, 90) involving either perturbation theory or numerical integration.

Woo & Roux (199) formalized the use of geometrical restraints acting on suitably chosen DOFs to narrow down the configurational space accessible to the binding partners as they associate and, thus, to ensure converged configurational ensemble averages. This pragmatic strategy has fueled the development of alternate approaches that are similar in spirit, such as funnel metadynamics (124, 154) and attach-pull-release (86), as well as several other restraints-based schemes in connection with alchemical transformations (50, 136, 188). From a numerical standpoint, restricting the accessible configurational space by means of geometrical restraints in the course of the physical separation is a standard variance-reduction strategy, with the tacit understanding that the contribution of the associated biasing potentials ought to be evaluated precisely at the two end states to supply the correct, unbiased estimate of the standard binding free energy (199). Generalization of the seminal work of Woo & Roux is embodied in the so-called alchemical and geometrical routes (83), whereby the different contributions to the binding affinity arising from the introduction of harmonic potentials acting on conformational, orientational, and positional CVs are accounted for through alchemical free-energy calculations—either FEP or TI—and PMF calculations, respectively (see **Figure 2**, **Supplemental Material**). Although computation of a radial separation PMF bereft of geometrical restraints can, in principle, yield valid results in the limit of sufficient sampling (179), in practice, introduction of such restraints accelerates the convergence of free-energy calculation by reducing the configurational space to be sampled. Yet determination of standard binding free energies relying on elements of the geometrical route, as well as several computational shortcuts, is not uncommon, despite an absence of formal justification (17, 56, 63, 72, 91, 93, 104, 117, 139, 145, 207). Both the alchemical and the geometrical routes have been applied successfully to a variety of protein–ligand complexes (65). In a proof of concept (83), it was shown that, although the two strategies yielded equally reliable free-energy estimates, computation of PMFs seemed somewhat more economical compared to its alchemical counterpart. In

Supplemental Material >

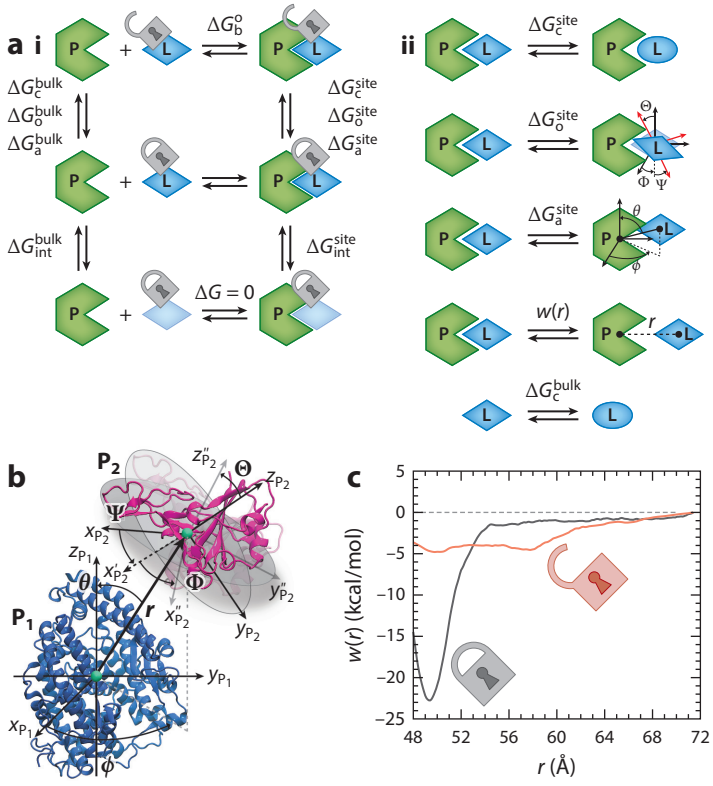

Figure 2

(*a*) Comparison between the alchemical (*i*) and the geometrical (*ii*) routes for the determination of the free energy, ΔG_b°, that characterizes the binding of a protein (P) and a ligand (L). (*b*) Collective variables utilized in the protein–protein binding free-energy calculation, illustrated in the cases of human angiotensin conversion enzyme 2 (ACE2) (P_1) and the SARS-CoV-2 receptor binding domain (RBD) (P_2). (*c*) Potential of mean force underlying the association of the RBD with ACE2 in the full geometrical route (*dark line*) and in the absence of restraints (*light line*).

general, however, the alchemical and the geometrical routes are not strictly speaking interchangeable, the former being better suited than the latter to buried substrates, albeit only when limited to small molecular objects. Only the geometrical route appears adapted to the determination of protein–protein binding free energies (82, 169). From the perspective of the practitioner, introduction of geometrical restraints to confine the guest with respect to the host in the course of the separation—or the decoupling of the binding partner—and estimation of their contribution to the standard binding free energy represent a cumbersome enterprise involving significant bookkeeping and computation of configurational integrals. To facilitate the determination of the binding affinity, several tools have been developed to streamline the protocol (65), from the setup of the free-energy calculations (66, 125, 202) to their posttreatment (66, 67).

The mosaic of developments for tackling the longstanding protein–ligand—and protein–protein—problem with an unassailable methodology has allowed the establishment of rigorous protocols (65, 154) for the computation of binding affinities of unprecedented reliability. However accomplished this methodology may be, it still remains vulnerable to several limitations, chief among which is its reliance on robust structural data, most notably the interface between the host

and the guest. Furthermore, convergence of the free-energy calculations at play is prone to be burdened by the possibility that the substrate undergoes conformational changes upon binding to the protein. From a computational standpoint, this shortcoming can be understood in terms of high barriers in orthogonal space, resulting in quasinonergodicity manifested in the unlikelihood of the substrate to isomerize as it is either coupled or decoupled from its environment. Importance-sampling algorithms are clearly insufficient to reflect the true conformational equilibrium; thus, the sampling enhancements described above are necessary to address the issue of kinetic traps (102, 200).

5. PASSIVE PERMEATION EVENTS ACROSS LIPID BILAYERS

A second fundamental molecular process is the permeation of chemical species across the biological membrane, which encapsulates the cell. The lipids that form the membrane are densely packed in bilayers to harbor the cell machinery and protect it from the environment while preserving ionic concentration gradients. Although the biological membrane constitutes an effective barrier against the spontaneous, unassisted permeation of ions and highly hydrophilic molecular compounds, passive diffusion of chemical species remains possible. The rate at which such permeation events are observed depends on the composition of the lipid bilayer and, thus, on its physical properties. In stark contrast with the assisted transport of molecular compounds—or permeants—across the membrane, which proceeds through highly selective integral proteins embedded in it, the selectivity of passive diffusion is rooted in the random fluctuations and intermolecular forces within the lipid environment. From a pharmaceutical perspective, prediction of passive permeation rates is of paramount importance, most notably for the delivery of lead candidates to their designated intracellular target and possibly for the subsequent excretion of metabolites. The impetus for this research comes from the likelihood that drug candidates exhibiting a strong affinity toward a given target can eventually be discarded owing to their acute cytotoxicity, mediocre bioavailability, or any other pharmacokinetic concern.

At the theoretical level, notwithstanding the importance of passive permeation for cell function, our mechanistic understanding of this molecular process is still largely fragmentary. To gain valuable insight while predicting the propensity of drug candidates to spontaneously traverse the biological membrane, experimental approaches aimed at measuring membrane permeability, like parallel artificial membrane permeability (PAMPA) (109) or cell-based CaCo-2 assays (8), have been utilized to train quantitative structure permeability relationship (QSPR) models (84). Although they are commonly employed in industrial settings, these inexpensive models have often proven poorly predictive, failing to supply reproducibly accurate information about passive diffusion across the membranes. An appealing route to capture the atomistic detail of permeation events while offering, in principle, a predictive picture of their underlying thermodynamics and kinetics consists of turning to numerical simulations, most notably MD. Strictly speaking, the membrane permeability, P_m, can be expressed as the ratio of the net flux of permeants crossing the lipid bilayer over the difference between their concentrations on each side of the bilayer. In other words, the rate of passive diffusion of the chemical species through the membrane possesses a thermodynamic component through these species' partition coefficient between the lipid and the aqueous phases and a kinetic one through the diffusivity of the permeant as it translocates across the aqueous interface.

Assuming equilibrium across the lipid bilayer, P_m can be defined in the framework of the inhomogeneous solubility-diffusivity model (9, 52) and depends exponentially on the PMF, $w(z)$, and linearly on the position-dependent diffusivity, $D(z)$ (see **Supplemental Material**). z is the projection onto the normal to the lipid bilayer of the Euclidian distance between the center of

Supplemental Material >

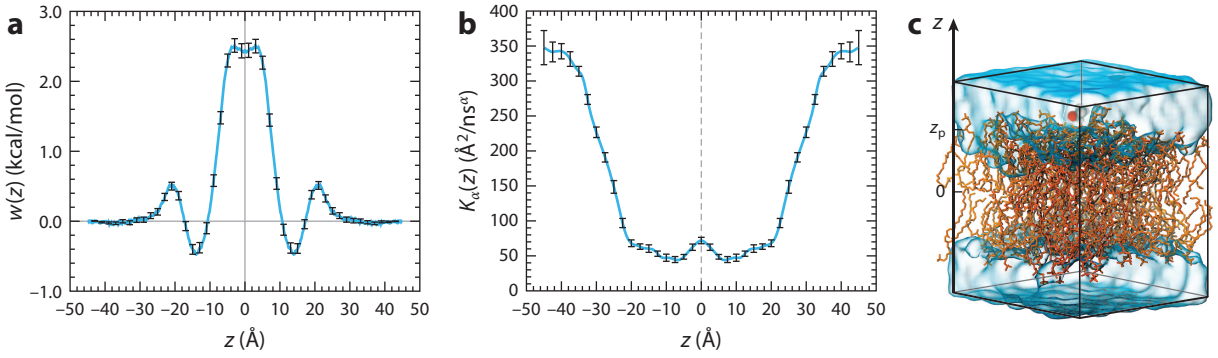

Figure 3

(*a*) Free energy profile, $w(z)$, and (*b*) position-dependent fractional diffusivity, $K_\alpha(z)$, underlying the permeation of ethanol across a fully hydrated 1-palmitoyl-2-oleoylphosphatidylcholine. (*c*) Computational assay utilized to determine $w(z)$ and $K_\alpha(z)$. The coarse variable, z, is the Euclidian distance between the center of mass of the bilayer and that of the permeant.

mass of the latter and that of the permeant (see **Figure 3**). As discussed below, choice of this ad hoc coarse variable, guided by intuition, raises conceptual difficulties in the description of the kinetics underlying the permeation event. Although determination of both $w(z)$ and $D(z)$ is, in principle, amenable to MD, assuming that all values of z are adequately sampled, the often large free-energy barriers against translocation of the permeant across the membrane makes passive permeation a rare event from a computational standpoint. For this reason, a variety of importance- and enhanced-sampling schemes have been employed to determine the free-energy change and the diffusivity of the permeant as a function of z. Among the popular algorithms, US (14, 26, 118, 155, 171), ABF (41–43, 68, 180, 181), metadynamics (76, 77), and their different variants have been applied with varying degrees of success to the computation of $w(z)$. Systematic comparison of US and ABF, with and without sampling enhancement by means of multiple copies, did not reveal any glaring advantage of preferring one algorithm over the others for the prediction of the membrane permeability to a series of small organic compounds (118). It ought to be mentioned, however, that persistence of hysteresis between the two sides of the lipid bilayer, when the homogeneity of the bilayer imposes a symmetrical free-energy profile, was observed over very long timescales, in excess of 4 μs, including for small permeants like urea. Slow convergence of the free-energy calculation is in large measure rooted in the choice of z as the transition coordinate, which is too rudimentary to account for the longtime relaxation of the acyl chains of the lipid bilayer. There is still one advantage of turning to gradient-based algorithms, like ABF, to determine $w(z)$, namely, the possibility of reconciling thermodynamics and kinetics at little additional cost and accessing the position-dependent diffusivity from the PMF calculation using Bayesian inferences (38). An alternative is provided by the generalized Langevin equation, which yields qualitatively similar results while underscoring a sensitivity to the choice of parameters, as well as membrane defects (118). An unfortunate consequence of the choice of z as a rudimentary order parameter is the failure of the probability of displacement of the permeant over sufficiently short time intervals to obey classical diffusion. In fact, for a variety of chemical species, the mean squared displacement along the normal to the membrane exhibits a power-law dependence of time, which is a hallmark of long-range spatiotemporal correlations (32). To account for this subdiffusive behavior, the motion of the permeant across the membrane should be modeled by means of a time-fractional Smoluchowski equation (32). A clarification is needed at this juncture—I do not suggest that, at a macroscopic

level, drug permeation across membranes is not diffusive. I merely note that turning to the time-fractional Smoluchowski equation is a consequence of a naive RC model and delusive assumption of timescale separation. It should also be clarified that importance-sampling algorithms combined with the inhomogeneous solubility-diffusion model do not constitute the only route toward the determination from first principles of the membrane permeability to chemical species. In fact, several alternate strategies, emancipated from the inhomogeneous solubility-diffusion model, have been explored, chief among which are methods relying on global observables, such as the crossing rate, the net flux across the membrane, and the difference in the permeant concentration on each side of the membrane. One such method is milestoning, whereby a large number of independent, unbiased short trajectories are spawned within compartmentalized regions of phase space to estimate individual transition rates between microstates and from whence the membrane permeability can be inferred. To a large extent, transition-based counting approaches are a particular embodiment of milestoning, with only two milestones coinciding with the aqueous interfaces, as opposed to a finer discretization scheme along the permeation pathway. It is reassuring to observe that, although they rest on fundamentally different foundations, membrane permeability calculations relying on several crossings, on the one hand, and on the determination of a PMF, on the other hand, can render a quantitatively similar picture of permeation events. As an example, the permeability of a 1-palmitoyl-2-oleoyl-phosphatidylcholine (POPC) bilayer to ethanol was 8.1×10^{-1} cm/s based on a 1.5-μs ABF simulation and the fractional inhomogeneous solubility-diffusion model (43); 0.9×10^{-1} cm/s based on a 140–ns biased-exchange MtD simulation (77); and $1.3–2.4 \times 10^{-1}$ cm/s based on crossing events and, respectively, 170 and 626 permeants (113).

6. WIDE-AMPLITUDE CONFORMATIONAL TRANSITIONS

The third molecular process examined in this review is the transition between conformational states, which is central to a host of functions fulfilled by the cell machinery. Such spatial transformations, which largely exceed milliseconds in complex biological objects, often consist of entangled movements of broad amplitude, which is likely to thwart their exploration over realistic timescales by means of atomistic computer simulations. The timescales amenable to MD, commonly from tens of microseconds on commodity clusters to a few milliseconds on special-purpose computers (163) and large arrays of computing nodes equipped with GPUs, remain orders of magnitude less than those spanned by these molecular processes. Yet observing through the computational microscope (57, 119) the broad movements between protein domains connected allosterically could be valuable to complement experiment and would certainly help address important biological questions, such as what happens between the binding of ATP^{4-} to the soluble V_1-domain of a vacuolar, V_OV_1-ATPase (62) and the rotation of the *c*-ring in the membrane V_O-domain, and between rotation and the subsequent release of a proton. The difficulty of answering such questions largely stems from conceptual and methodological obstacles rooted in the identification of the DOFs at play and their representation by a suitable set of CVs, on the one hand, and the choice of algorithm that encourages sampling along these CVs, on the other hand. These obstacles have admittedly limited the number of discoveries made by theory in important objects of the cell machinery. Considering the intricacy of the molecular process at hand, envisaging its exploration through the narrow prism of free-energy calculations alone is unlikely to be successful, regardless of the numerical efficiency of the importance-sampling algorithm. Why is this the case? As is discussed at length above, enhancing sampling to investigate phenomena spanning long timescales is commonly achieved by defining a surrogate of the RC, $\xi(\mathbf{x})$, and encouraging exploration of important regions of configurational space through the variety of numerical schemes outlined in this review (39, 48, 61, 95, 115, 175, 178, 186, 206). However astute these

schemes might be, they remain vulnerable to timescale separation and misrepresentation of the RC, which result in sampling nonuniformity in the direction of $\xi(\mathbf{x})$. Returning to the example of V_OV_1-ATPase, it is plainly impossible to infer the CVs responsible for the conformational transition between two intermediate states of a catalytic step by merely comparing with the human eye the associated structures. The strong connection between the algorithm encouraging sampling of important regions (34, 120) and the representation of $\xi(\mathbf{x})$ necessarily impacts not only sampling efficacy, but also the underlying dynamics. This connection naturally raises the question of what constitutes a suitable set of CVs, or, said differently, what are the important DOFs that contribute predominantly to $\xi(\mathbf{x})$, a longstanding question that has prompted the development of a host of approaches that cannot all be cited in this review (3, 6, 13, 19, 21, 28, 30, 61, 138, 140, 143, 146, 149, 177, 190, 192, 193). Historically, development of algorithms to model the RC—subsuming identification of CVs—and development of sampling algorithms have been rather compartmented research areas (34).

In the context of importance-sampling strategies relying on the definition of a model RC discretized in infinitesimal bins, as, for instance, in the ABF (39, 48) or US (178) families of algorithms, current technological hurdles, notably limited access to large amounts of memory, preclude sampling the CV subspace beyond a dimension of three. A practical solution to circumvent this limitation consists of keeping the CV space multidimensional while sampling only around a particular pathway, represented by a curvilinear abscissa, $\xi(s)$, function of scalar $s \in [0, 1]$. One possible route to identify this pathway connecting two metastable states of the free-energy landscape is provided by the string method (127, 193). It represents $\xi(s)$ as a chain of discrete intermediate states, or images, in the subspace of the CVs—or, alternatively, of the Cartesian coordinates when no obvious CVs can be identified. Its popular variant, the string method with swarms of trajectories (SMwST) (29, 143), iteratively refines a trial curvilinear abscissa on the basis of the average dynamic local drift determined from multiple short, unbiased trajectories spawned at each node. Convergence of the optimization is attained when the local drift at each node is zero in directions orthogonal to the tangent of the pathway—thus, this is called the zero-drift pathway (ZDP). Contrary to common beliefs, the ZDP is not the MPTP, let alone the minimum free-energy pathway (29). To ascertain whether the curvilinear abscissa supplied by the SMwST corresponds, indeed, to the MPTP, it is critical to explore alternate ZDPs by considering distinct trial pathways, as well as randomization schemes. The MPTP is the ZDP that has the highest rate constant, or the shortest mean first passage time (172), determined, for instance, using Bayesian inferences (38).

With a physically meaningful pathway that connects the conformational states of interest, the free energy can then be mapped by encouraging sampling in the relevant regions, following the strategies described above. US, in its different flavors, has been employed on a variety of biological objects and molecular processes, ranging from the activation of pronto-oncogene c-Src kinase (60, 131) to the substrate-induced conformational transition of membrane carriers (137, 138) and of a glucose transporter (110), the opening of a pentameric ligand-gated channel (123), and the rotary-catalysis step of the V_1-domain of a V_OV_1-ATPase (167). Conformational changes have also been investigated, combining path-searching methods and MtD, for instance, in the case of G protein–coupled receptor activation (153) and of ligand-induced open-to-closed transition in cyclin-dependent kinases (16). These simulations rest on the introduction of path-CVs (PCVs) (23, 29, 53, 92), which allow the free energy to be determined along $\xi(s)$. PCVs are well suited to sampling strategies leaning on the computation of a local mean force and have been used in the challenging example of the auto-inhibited V_O-domain of a V_OV_1-ATPase (158) (see **Figure 4**). The combination of path-searching techniques and importance-sampling algorithms is not limited to these few remarkable illustrations. Other strategies also exist, such as ABP optimization in the CV subspace associated with unrestricted, enhanced sampling along the transition pathway

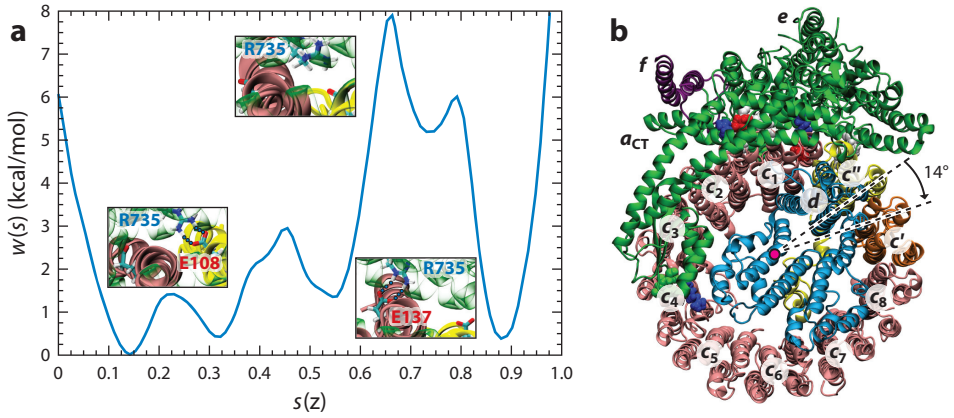

Figure 4

(*a*) Free-energy profile underlying the clockwise 14°-rotation of an auto-inhibited V_O-domain *c*-ring from a V_OV_1-ATPase (c″E108), determined along a pathway optimized using the string method with swarms of trajectories. (*b*) Detail of the auto-inhibited V_O-domain and its different subdomains.

(54). Notwithstanding significant efforts to decrypt these complex molecular processes by means of computer simulations, applications to large, 10^5-atom-scale objects of the cell machinery have hitherto remained scarce. This paucity of large-scale path-following free-energy calculations can be explained, at least in part, by the considerable computer times, in excess of microseconds (158, 167), involved, on the one hand, in the identification of the transition pathway and, on the other hand, in the determination of the free-energy change along this transition pathway. The staggering computational investment magnified by the necessity of distinguishing the MPTP amid alternate ZDPs provides an impetus for forging effective workflows and tools that are well suited to large biological objects.

7. SUMMARY

Although it is generally accepted that free-energy calculations have come of age to help understand a variety of molecular processes relevant to biophysics, their predictive power is often called into question, most notably for qualitatively new problems. This legitimate skepticism can be explained, at least in part, by the conceptual and practical difficulties of bridging the gaping divide between the phenomena observed experimentally at the macroscopic level and how we model them at the microscopic level. Reconciling size and timescales to render a faithful picture of the biological reality presupposes our ability to address timescale separation—and, thus, to identify the relevant DOFs at play—which remains a major hurdle, notwithstanding access to computer architectures equipped with hundreds of GPUs. In many instances, our intuition is not enough, and however smart the free-energy method is, it remains plagued by quasinonergodicity scenarios, emphasizing the need to resort to dedicated approaches to model the RC. Inclination to skepticism can also be rationalized by an ever-expanding methodological palette and the difficulty of making an informed choice of the algorithm best adapted to decipher the molecular process of interest. One attractive feature of free-energy calculations lies in the possibility to combine algorithms seamlessly to improve ergodic sampling. The sophistication of force fields (121, 151), now able to reproduce thermodynamic quantities with unprecedented accuracy, has created an impetus for novel ideas to overcome the last roadblocks that have hitherto hampered the exploration of rare events. As original theoretical frameworks designed for more reliable

free-energy estimates continue to emerge, it is also crucial to push the methodology to its limits with challenging tests. Ten similar reviews would not be enough to quote the legion of research articles applying free-energy calculations. Still, exercises like the SAMPL series of blind predictions of host–guest binding affinities, pK_as, and partition coefficients (79) provide a fair account of the current state of the art and where the field is going. Similar initiatives eliciting joint efforts in the community ought to be encouraged to craft the next generation of sampling strategies supplying free-energy estimates with improved reliability.

DISCLOSURE STATEMENT

The author is not aware of any affiliations, memberships, funding, or financial holdings that might be perceived as affecting the objectivity of this review.

ACKNOWLEDGMENTS

This work was supported by the Agence Nationale de la Recherche (grants LOR–AI and ProteaseInAction). I am particularly indebted to James C. Gumbart, Mahmoud Moradi, and Christopher Rowley for critical reading of this review. I apologize in advance to the many authors of excellent research articles that I could not cite owing to page limits.

LITERATURE CITED

1. Abraham MJ, Murtola T, Schulz R, Páll S, Smith JC, et al. 2015. GROMACS: high performance molecular simulations through multi-level parallelism from laptops to supercomputers. *SoftwareX* 1–2:19–25
2. Abrams C, Bussi G. 2014. Enhanced sampling in molecular dynamics using metadynamics, replica-exchange, and temperature-acceleration. *Entropy* 16:163–99
3. Ahmad M, Helms V, Kalinina OV, Lengauer T. 2019. Relative principal components analysis: application to analyzing biomolecular conformational changes. *J. Chem. Theory Comput.* 15:2166–78
4. Aldeghi M, Heifetz A, Bodkin MJ, Knapp S, Biggin PC. 2016. Accurate calculation of the absolute free energy of binding for drug molecules. *Chem. Sci.* 7(1):207–18
5. Alder BJ, Wainwright TE. 1957. Phase transition for a hard sphere systems. *J. Chem. Phys.* 27:1208–9
6. Amadei A, Linssen AB, Berendsen HJ. 1993. Essential dynamics of proteins. *Proteins* 17:412–25
7. Ando T. 2014. High-speed AFM imaging. *Curr. Opin. Struct. Biol.* 28:63–68
8. Artursson P, Palm K, Luthman K. 2001. Caco-2 monolayers in experimental and theoretical predictions of drug transport. *Adv. Drug Deliv. Rev.* 46:27–43
9. Awoonor-Williams E, Rowley CN. 2015. Molecular simulation of nonfacilitated membrane permeation. *Biochim. Biophys. Acta Biomembr.* 1858:1672–87
10. Barducci A, Bussi G, Parrinello M. 2008. Well-tempered metadynamics: a smoothly converging and tunable free-energy method. *Phys. Rev. Lett.* 100:020603
11. Bartels C, Karplus M. 1997. Multidimensional adaptive umbrella sampling: applications to main chain and side chain peptide conformations. *J. Comput. Chem.* 18:1450–62
12. Bash PA, Singh UC, Langridge R, Kollman PA. 1987. Free energy calculations by computer simulation. *Science* 236:564–68
13. Belkacemi Z, Gkeka P, Lelièvre T, Stoltz G. 2022. Chasing collective variables using autoencoders and biased trajectories. *J. Chem. Theory Comput.* 18(1):59–78
14. Bemporad D, Luttmann C, Essex JW. 2004. Computer simulation of small molecule permeation across a lipid bilayer: dependence on bilayer properties and solute volume, size, and cross-sectional area. *Biophys. J.* 87:1–13
15. Bennett CH. 1976. Efficient estimation of free energy differences from Monte Carlo data. *J. Comp. Phys.* 22:245–68

16. Bešker N, Gervasio FL. 2012. Using metadynamics and path collective variables to study ligand binding and induced conformational transitions. *Methods Mol. Biol.* 819:501–13
17. Blazhynska M, Goulard Coderc de Lacam E, Chen H, Roux B, Chipot C. 2022. Hazardous shortcuts in standard binding free-energy calculations. *J. Phys. Chem. Lett.* 13(27):6250–58
18. Bolhuis PG, Chandler D, Dellago C, Geissler P. 2002. Transition path sampling: throwing ropes over mountain passes, in the dark. *Ann. Rev. Phys. Chem.* 59:291–318
19. Bolhuis PG, Dellago C, Chandler D. 2000. Reaction coordinates of biomolecular isomerization. *PNAS* 97:5877–82
20. Boresch S, Tettinger F, Leitgeb M, Karplus M. 2003. Absolute binding free energies: a quantitative approach to their calculation. *J. Phys. Chem. B* 107:9535–51
21. Bowman GR, Pande VS, Noé F. 2013. *An Introduction to Markov State Models and Their Application to Long Timescale Molecular Simulation*. Adv. Exp. Med. Biol. 797. Berlin: Springer
22. Boyce SE, Mobley DL, Rocklin GJ, Graves AP, Dill KA, Shoichet BK. 2009. Predicting ligand binding affinity with alchemical free energy methods in a polar model binding site. *J. Mol. Biol.* 394:747–63
23. Branduardi D, Gervasio FL, Parrinello M. 2007. From A to B in free energy space. *J. Chem. Phys.* 126:054103
24. Buch I, Giorgino T, Fabritiis GD. 2011. Complete reconstruction of an enzyme-inhibitor binding process by molecular dynamics simulations. *PNAS* 108:10184–89
25. Bussi G, Gervasio FL, Laio A, Parrinello M. 2006. Free-energy landscape for β hairpin folding from combined parallel tempering and metadynamics. *J. Am. Chem. Soc.* 128(41):13435–41
26. Carpenter TS, Kirshner DA, Lau EY, Wong SE, Nilmeier JP, Lightstone FC. 2014. A method to predict blood-brain barrier permeability of drug-like compounds using molecular dynamics simulations. *Biophys. J.* 107(3):630–41
27. Chen H, Fu H, Chipot C, Shao X, Cai W. 2021. Overcoming free-energy barriers with a seamless combination of a biasing force and collective variable-independent boost potential. *J. Chem. Theory Comput.* 17:3886–94
28. Chen H, Liu H, Feng H, Fu H, Cai W, et al. 2022. MLCV: bridging machine-learning-based dimensionality reduction and free-energy calculation. *J. Chem. Inf. Model.* 62:1–8
29. Chen H, Ogden D, Pant S, Roux B, Moradi M, et al. 2022. A companion guide to the string method with swarms of trajectories, characterization, performance, and pitfalls. *J. Chem. Theory Comput.* 18:1406–22
30. Chen W, Tan AR, Ferguson AL. 2018. Collective variable discovery and enhanced sampling using autoencoders: innovations in network architecture and error function design. *J. Chem. Phys.* 149(7):072312
31. Chipot C. 2014. Frontiers in free-energy calculations of biological systems. *Wiley Interdiscip. Rev. Comput. Mol. Sci.* 4:71–89
32. Chipot C, Comer J. 2016. Subdiffusion in membrane permeation of small molecules. *Sci. Rep.* 6:35913
33. Chipot C, Lelièvre T. 2011. Enhanced sampling of multidimensional free-energy landscapes using adaptive biasing forces. *SIAM J. Appl. Math.* 71:1673–95
34. Chipot C, Pohorille A, eds. 2007. *Free Energy Calculations: Theory and Applications in Chemistry and Biology*. Berlin: Springer
35. Chodera JD, Mobley DL, Shirts MR, Dixon RW, Branson K, Pande VS. 2011. Alchemical free energy methods for drug discovery: progress and challenges. *Curr. Opin. Struct. Biol.* 21:150–60
36. Chodera JD, Noé F. 2014. Markov state models of biomolecular conformational dynamics. *Curr. Opin. Struct. Biol.* 25:135–44
37. Christ CD, van Gunsteren WF. 2007. Enveloping distribution sampling: a method to calculate free energy differences from a single simulation. *J. Chem. Phys.* 126:184110
38. Comer J, Chipot C, González-Nilo FD. 2013. Calculating position-dependent diffusivity in biased molecular dynamics simulations. *J. Chem. Theor. Comput.* 9:876–82
39. Comer J, Gumbart JC, Hénin J, Lelièvre T, Pohorille A, Chipot C. 2015. The adaptive biasing force method: everything you always wanted to know, but were afraid to ask. *J. Phys. Chem. B* 119:1129–51
40. Comer J, Phillips J, Schulten K, Chipot C. 2014. Multiple-replica strategies for free-energy calculations in NAMD: multiple-walker adaptive biasing force and walker selection rules. *J. Chem. Theor. Comput.* 10:5276–85

41. Comer J, Schulten K, Chipot C. 2014. Calculation of lipid-bilayer permeabilities using an average force. *J. Chem. Theory Comput.* 10:554–64
42. Comer JR, Schulten K, Chipot C. 2014. Diffusive models of membrane permeation with explicit orientational freedom. *J. Chem. Theory Comput.* 10:2710–18
43. Comer J, Schulten K, Chipot C. 2017. Permeability of a fluid lipid bilayer to short-chain alcohols from first principles. *J. Chem. Theory Comput.* 13(6):2523–32
44. Cournia Z, Allen B, Sherman W. 2017. Relative binding free energy calculations in drug discovery: recent advances and practical considerations. *J. Chem. Inf. Model.* 57(12):2911–37
45. Cournia Z, Chipot C, Roux B, York DM, Sherman W. 2021. Free energy methods in drug discovery—introduction. In *Free Energy Methods in Drug Discovery: Current State and Future Directions*, ed. K Armacost, D Thompson, pp. 267–87. ACS Symp. Ser. 1397. Washington, DC: Am. Chem. Soc.
46. Crooks G. 1998. Nonequilibrium measurements of free energy differences for microscopically reversible Markovian systems. *J. Stat. Phys.* 90:1481–87
47. Dama JF, Parrinello M, Voth GA. 2014. Well-tempered metadynamics converges asymptotically. *Phys. Rev. Lett.* 112(24):240602
48. Darve E, Pohorille A. 2001. Calculating free energies using average force. *J. Chem. Phys.* 115:9169–83
49. De Donder T. 1927. *L'Affinité*. Paris: Gauthier–Villars
50. Deng Y, Roux B. 2006. Calculation of standard binding free energies: aromatic molecules in the T4 lysozyme L99A mutant. *J. Chem. Theor. Comp.* 2:1255–73
51. Deng Y, Roux B. 2009. Computations of standard binding free energies with molecular dynamics simulations. *J. Phys. Chem. B* 113:2234–46
52. Diamond JM, Katz Y. 1974. Interpretation of nonelectrolyte partition coefficients between dimyristoyl lecithin and water. *J. Membrane Biol.* 17:121–54
53. Díaz Leines G, Ensing B. 2012. Path finding on high-dimensional free energy landscapes. *Phys. Rev. Lett.* 109(2):020601
54. Dickson BM, Huang H, Post CB. 2012. Unrestrained computation of free energy along a path. *J. Phys. Chem. B* 116(36):11046–55
55. Dixit SB, Chipot C. 2001. Can absolute free energies of association be estimated from molecular mechanical simulations? The biotin–streptavidin system revisited. *J. Phys. Chem. A* 105:9795–99
56. Doudou S, Burton NA, Henchman RH. 2009. Standard free energy of binding from a one-dimensional potential of mean force. *J. Chem. Theor. Comput.* 5:909–18
57. Dror RO, Dirks RM, Grossman JP, Xu H, Shaw DE. 2012. Biomolecular simulation: a computational microscope for molecular biology. *Annu. Rev. Biophys.* 41:429–52
58. Dror RO, Pan AC, Arlow DH, Borhani DW, Maragakis P, et al. 2011. Pathway and mechanism of drug binding to G-protein-coupled receptors. *PNAS* 108:13118–23
59. Eastman P, Swails J, Chodera JD, McGibbon RT, Zhao Y, et al. 2017. Openmm 7: rapid development of high performance algorithms for molecular dynamics. *PLOS Comput. Biol.* 13(7):e1005659
60. Fajer M, Meng Y, Roux B. 2017. The activation of c-Src tyrosine kinase: conformational transition pathway and free energy landscape. *J. Phys. Chem. B* 121(15):3352–63
61. Faradjian AK, Elber R. 2004. Computing time scales from reaction coordinates by milestoning. *J. Chem. Phys.* 120:10880–89
62. Forgac M. 2007. Vacuolar ATPases rotary proton pumps in physiology and pathophysiology. *Nat. Rev. Mol. Cell Biol.* 8(11):917–29
63. Francés-Monerris A, Hognon C, Miclot T, García-Iriepa C, Iriepa I, et al. 2020. Molecular basis of SARS-CoV-2 infection and rational design of potential antiviral agents: modeling and simulation approaches. *J. Proteome Res.* 19(11):4291–315
64. Frenkel D, Smit B. 1996. *Understanding Molecular Simulations: From Algorithms to Applications*. San Diego: Acad. Press
65. Fu H, Chen H, Blazhynska M, Goulard Coderc De Lacam E, Szczepaniak F, et al. 2022. Accurate determination of protein:ligand standard binding free energies from molecular dynamics simulations. *Nat. Protoc.* 17:1114–41
66. Fu H, Chen H, Cai W, Shao X, Chipot C. 2021. BFEE2: automated, streamlined and accurate absolute binding free-energy calculations. *J. Chem. Inf. Model.* 61:2116–23

67. Fu H, Gumbart JC, Chen H, Shao X, Cai W, Chipot C. 2018. BFEE: a user-friendly graphical interface facilitating absolute binding free-energy calculations. *J. Chem. Inf. Model.* 58:556–60
68. Fu H, Shao X, Cai W, Chipot C. 2019. Taming rugged free-energy landscapes using an average force. *Acc. Chem. Res.* 52:3254–64
69. Fu H, Shao X, Chipot C, Cai W. 2016. Extended adaptive biasing force algorithm: an on-the-fly implementation for accurate free-energy calculations. *J. Chem. Theory Comput.* 12:3506–13
70. Fujitani H, Tanida Y, Ito M, Jayachandran G, Snow CD, et al. 2005. Direct calculation of the binding free energies of FKBP ligands. *J. Chem. Phys.* 123:084108
71. Gao J, Kuczera K, Tidor B, Karplus M. 1989. Hidden thermodynamics of mutant proteins: a molecular dynamics analysis. *Science* 244:1069–72
72. García-Iriepa C, Hognon C, Francés-Monerris A, Iriepa I, Miclot T, et al. 2020. Thermodynamics of the interaction between the spike protein of severe acute respiratory syndrome coronavirus-2 and the receptor of human angiotensin-converting enzyme 2: effects of possible ligands. *J. Phys. Chem. Lett.* 11(21):9272–81
73. General IJ, Dragomirova R, Meirovitch H. 2011. Calculation of the absolute free energy of binding and related entropies with the HSMD-TI method: the FKBP12-L8 complex. *J. Chem. Theory Comput.* 7:4196–207
74. General IJ, Dragomirova R, Meirovitch H. 2011. New method for calculating the absolute free energy of binding: the effect of a mobile loop on the avidin/biotin complex. *J. Phys. Chem. B* 115:168–75
75. General IJ, Dragomirova R, Meirovitch H. 2012. Absolute free energy of binding of avidin/biotin, revisited. *J. Phys. Chem. B* 116:6628–36
76. Ghaemi Z, Alberga D, Carloni P, Laio A, Lattanzi G. 2016. Permeability coefficients of lipophilic compounds estimated by computer simulations. *J. Chem. Theory Comput.* 12(8):4093–99
77. Ghaemi Z, Minozzi M, Carloni P, Laio A. 2012. A novel approach to the investigation of passive molecular permeation through lipid bilayers from atomistic simulations. *J. Phys. Chem. B* 116:8714–21
78. Gilson MK, Given JA, Bush BL, McCammon JA. 1997. The statistical–thermodynamic basis for computation of binding affinities: a critical review. *Biophys. J.* 72:1047–69
79. Grosjean H, Işik M, Aimon A, Mobley D, Chodera J, et al. 2022. SAMPL7 protein-ligand challenge: a community-wide evaluation of computational methods against fragment screening and pose-prediction. *J. Comput.-Aided Mol. Des.* 36(4):291–311
80. Grubmüller H. 1995. Predicting slow structural transitions in macromolecular systems: conformational flooding. *Phys. Rev. E* 52(3):2893–906
81. Grubmüller H, Heymann B, Tavan P. 1996. Ligand binding: molecular mechanics calculation of the streptavidin–biotin rupture force. *Science* 271:997–99
82. Gumbart JC, Roux B, Chipot C. 2013. Efficient determination of protein-protein standard binding free energies from first principles. *J. Chem. Theor. Comput.* 9:3789–98
83. Gumbart JC, Roux B, Chipot C. 2013. Standard binding free energies from computer simulations: What is the best strategy? *J. Chem. Theor. Comput.* 9:794–802
84. Hansch C, Dunn WJ III. 1972. Linear relationships between lipophilic character and biological activity of drugs. *J. Pharm. Sci.* 61:1–19
85. Harger M, Li D, Wang Z, Dalby K, Lagardère L, et al. 2017. Tinker-OpenMM: absolute and relative alchemical free energies using AMOEBA on GPUs. *J. Comput. Chem.* 38(23):2047–55
86. Heinzelmann G, Henriksen NM, Gilson MK. 2017. Attach-pull-release calculations of ligand binding and conformational changes on the first BRD4 bromodomain. *J. Chem. Theory Comput.* 13(7):3260–75
87. Hénin J. 2021. Fast and accurate multidimensional free energy integration. *J. Chem. Theory Comput.* 17(11):6789–98
88. Hénin J, Chipot C. 2004. Overcoming free energy barriers using unconstrained molecular dynamics simulations. *J. Chem. Phys.* 121:2904–14
89. Hermans J, Shankar S. 1986. The free energy of xenon binding to myoglobin from molecular-dynamics simulation. *Isr. J. Chem.* 27:225–27
90. Hermans J, Wang L. 1997. Inclusion of loss of translational and rotational freedom in theoretical estimates of free energies of binding: application to a complex of benzene and mutant T4 lysozyme. *J. Am. Chem. Soc.* 119:2707–14

91. Hernández-Alvarez L, Oliveira AB, Hernández-González JE, Chahine J, Pascutti PG, et al. 2021. Computational study on the allosteric mechanism of *Leishmania major* IF4E-1 by 4E-interacting protein-1: unravelling the determinants of m^7GTP cap recognition. *Comput. Struct. Biotechnol. J.* 19:2027–44
92. Hovan L, Comitani F, Gervasio FL. 2019. Defining an optimal metric for the path collective variables. *J. Chem. Theory Comput.* 15(1):25–32
93. Hu F, Liu XT, Zhang JL, Zheng QC, Eglitis RI, Zhang HX. 2019. MD simulation investigation on the binding process of smoke-derived germination stimulants to its receptor. *J. Chem. Inf. Model.* 59(4):1554–62
94. Huang D, Caflisch A. 2004. Efficient evaluation of binding free energy using continuum electrostatics solvation. *J. Med. Chem.* 47:5791–97
95. Huber GA, Kim S. 1996. Weighted-ensemble Brownian dynamics simulations for protein association reactions. *Biophys. J.* 70(1):97–110
96. Huber T, Torda AE, van Gunsteren WF. 1994. Local elevation: a method for improving the searching properties of molecular dynamics simulation. *J. Comput.-Aided Mol. Des.* 8:695–708
97. Invernizzi M, Parrinello M. 2020. Rethinking metadynamics: from bias potentials to probability distributions. *J. Phys. Chem. Lett.* 11(7):2731–36
98. Izrailev S, Stepaniants S, Isralewitz B, Kosztin D, Lu H, et al. 1998. Steered molecular dynamics. In *Computational Molecular Dynamics: Challenges, Methods, Ideas*, ed. P Deuflhard, J Hermans, B Leimkuhler, AE Mark, R Skeel, S Reich, pp. 39–65. Lect. Notes Comput. Sci. Eng. 4. Berlin: Springer
99. Jarzynski C. 1997. Nonequilibrium equality for free energy differences. *Phys. Rev. Lett.* 78:2690–93
100. Jiang W, Hodoscek M, Roux B. 2009. Computation of absolute hydration and binding free energy with free energy perturbation distributed replica-exchange molecular dynamics. *J. Chem. Theory Comput.* 5:2583–88
101. Jiang W, Phillips J, Huang L, Fajer M, Meng Y, et al. 2014. Generalized scalable multiple copy algorithms for molecular dynamics simulations in NAMD. *Comput. Phys. Commun.* 185:908–16
102. Jiang W, Roux B. 2010. Free energy perturbation Hamiltonian replica-exchange molecular dynamics (FEP/H–REMD) for absolute ligand binding free energy calculations. *J. Chem. Theory Comput.* 6:2559–65
103. Jiao D, Golubkov PA, Darden TA, Ren P. 2008. Calculation of protein-ligand binding free energy by using a polarizable potential. *PNAS* 105:6290–95
104. Jin X, Bai Q, Xue W, Liu H, Yao X. 2015. Computational study on the inhibition mechanism of a cyclic peptide MaD5 to PfMATE: insight from molecular dynamics simulation, free energy calculation and dynamical network analysis. *Chemom. Intell. Lab. Syst.* 149:81–88
105. Jorgensen WL. 1989. Free-energy calculations: a breakthrough for modeling organic chemistry in solutions. *Acc. Chem. Res.* 22:184–89
106. Jorgensen WL, Buckner JK, Boudon S, Tirado-Rives J. 1988. Efficient computation of absolute free energies of binding by computer simulations: application to the methane dimer in water. *J. Chem. Phys.* 89:3742–46
107. Jorgensen WL, Ravimohan C. 1985. Monte Carlo simulation of differences in free energies of hydration. *J. Chem. Phys.* 83:3050–54
108. Jorgensen WL, Thomas LL. 2008. Perspective on free-energy perturbation calculations for chemical equilibria. *J. Chem. Theory Comput.* 4(6):869–76
109. Kansy M, Senner F, Gubernator K. 1998. Physicochemical high throughput screening: parallel artificial membrane permeation assay in the description of passive absorption processes. *J. Med. Chem.* 41:1007–10
110. Ke M, Yuan Y, Jiang X, Yan N, Gong H. 2017. Molecular determinants for the thermodynamic and functional divergence of uniporter GLUT1 and proton symporter XylE. *PLOS Comput. Biol.* 13(6):e1005603
111. Kirkwood JG. 1935. Statistical mechanics of fluid mixtures. *J. Chem. Phys.* 3:300–13
112. Kollman PA. 1993. Free energy calculations: applications to chemical and biochemical phenomena. *Chem. Rev.* 93:2395–417
113. Krämer A, Ghysels A, Wang E, Venable RM, Klauda JB, et al. 2020. Membrane permeability of small molecules from unbiased molecular dynamics simulations. *J. Chem. Phys.* 153(12):124107

114. Kumar S, Bouzida D, Swendsen RH, Kollman PA, Rosenberg JM. 1992. The weighted histogram analysis method for free energy calculations on biomolecules. I. The method. *J. Comput. Chem.* 13:1011–21
115. Laio A, Parrinello M. 2002. Escaping free energy minima. *PNAS* 99:12562–65
116. Landau LD. 1938. *Statistical Physics*. Oxford, UK: Clarendon Press
117. Lapelosa M. 2018. Conformational dynamics and free energy of BHRF1 binding to Bim BH3. *Biophys. Chem.* 232:22–28
118. Lee CT, Comer J, Herndon C, Leung N, Pavlova A, et al. 2016. Simulation-based approaches for determining membrane permeability of small compounds. *J. Chem. Inf. Model.* 56:721–33
119. Lee EH, Hsin J, Sotomayor M, Comellas G, Schulten K. 2009. Discovery through the computational microscope. *Structure* 17:1295–306
120. Lelièvre T, Stoltz G, Rousset M. 2010. *Free Energy Computations: A Mathematical Perspective*. London: Imp. Coll. Press
121. Lemkul JA, Huang J, Roux B, MacKerell AD. 2016. An empirical polarizable force field based on the classical Drude oscillator model: development history and recent applications. *Chem. Rev.* 116(9):4983–5013
122. Lesage A, Lelièvre T, Stoltz G, Hénin J. 2017. Smoothed biasing forces yield unbiased free energies with the extended-system adaptive biasing force method. *J. Phys. Chem. B* 121(15):3676–85
123. Lev B, Murail S, Poitevin F, Cromer BA, Baaden M, et al. 2017. String method solution of the gating pathways for a pentameric ligand-gated ion channel. *PNAS* 114(21):E4158–67
124. Limongelli V, Bonomi M, Parrinello M. 2013. Funnel metadynamics as accurate binding free-energy method. *PNAS* 110(16):6358–63
125. Loeffler HH, Michel J, Woods C. 2015. FESetup: automating setup for alchemical free energy simulations. *J. Chem. Inf. Model.* 55(12):2485–90
126. Maragakis P, Spichty M, Karplus M. 2006. Optimal estimates of free energies from multistate nonequilibrium work data. *Phys. Rev. Lett.* 96:100602
127. Maragliano L, Vanden-Eijnden E. 2006. A temperature accelerated method for sampling free energy and determining reaction pathways in rare events simulations. *Chem. Phys. Lett.* 426:168–75
128. Marsili S, Barducci A, Chelli R, Procacci P, Schettino V. 2006. Self–healing umbrella sampling: a non–equilibrium approach for quantitative free energy calculations. *J. Phys. Chem. B* 110:14011–13
129. McCammon JA, Gelin BR, Karplus M. 1977. Dynamics of folded proteins. *Nature* 267:585–90
130. McDonald IR, Singer K. 1967. Calculation of thermodynamic properties of liquid argon from Lennard-Jones parameters by a Monte Carlo method. *Discuss. Faraday Soc.* 43:40–49
131. Meng Y, Lin Y, Roux B. 2015. Computational study of the "DFG-flip" conformational transition in c-Abl and c-Src tyrosine kinases. *J. Phys. Chem. B* 119(4):1443–56
132. Miao Y, Feher VA, McCammon JA. 2015. Gaussian accelerated molecular dynamics: unconstrained enhanced sampling and free energy calculation. *J. Chem. Theory Comput.* 11(8):3584–95
133. Minoukadeh K, Chipot C, Lelièvre T. 2010. Potential of mean force calculations: a multiple-walker adaptive biasing force approach. *J. Chem. Theory Comput.* 6:1008–17
134. Mitsutake A, Sugita Y, Okamoto Y. 2001. Generalized-ensemble algorithms for molecular simulations of biopolymers. *Biopolymers* 60(2):96–123
135. Miyamoto S, Kollman PA. 1993. What determines the strength of noncovalent association of ligands to proteins in aqueous solution ? *PNAS* 90:8402–6
136. Mobley DL, Graves AP, Chodera JD, McReynolds AC, Shoichet BK, Dill KA. 2007. Predicting absolute ligand binding free energies to a simple model site. *J. Mol. Biol.* 371:1118–34
137. Moradi M, Enkavi G, Tajkhorshid E. 2015. Atomic-level characterization of transport cycle thermodynamics in the glycerol-3-phosphate:phosphate antiporter. *Nat. Commun.* 6:8393
138. Moradi M, Tajkhorshid E. 2013. Mechanistic picture for conformational transition of a membrane transporter at atomic resolution. *PNAS* 110:18916–21
139. Niu Y, Shi D, Li L, Guo J, Liu H, Yao X. 2017. Revealing inhibition difference between PFI-2 enantiomers against SETD7 by molecular dynamics simulations, binding free energy calculations and unbinding pathway analysis. *Sci. Rep.* 7:46547

140. Noé F, Olsson S, Köhler J, Wu H. 2019. Boltzmann generators: sampling equilibrium states of many-body systems with deep learning. *Science* 365(6457):eaaw1147
141. Onsager L. 1938. Initial recombination of ions. *Phys. Rev.* 54(8):554–57
142. Oshima H, Re S, Sugita Y. 2019. Replica-exchange umbrella sampling combined with Gaussian accelerated molecular dynamics for free-energy calculation of biomolecules. *J. Chem. Theory Comput.* 15(10):5199–208
143. Pan AC, Sezer D, Roux B. 2008. Finding transition pathways using the string method with swarms of trajectories. *J. Phys. Chem. B* 112:3432–40
144. Park S, Khalili-Araghi F, Tajkhorshid E, Schulten K. 2003. Free energy calculation from steered molecular dynamics simulations using Jarzynski's equality. *J. Chem. Phys.* 119:3559–66
145. Patel JS, Ytreberg FM. 2018. Fast calculation of protein-protein binding free energies using umbrella sampling with a coarse-grained model. *J. Chem. Theory Comput.* 14(2):991–97
146. Pérez-Hernández G, Paul F, Giorgino T, De Fabritiis G, Noé F. 2013. Identification of slow molecular order parameters for Markov model construction. *J. Chem. Phys.* 139:015102
147. Phillips JC, Hardy DJ, Maia JDC, Stone JE, Ribeiro JV, et al. 2020. Scalable molecular dynamics on CPU and GPU architectures with NAMD. *J. Chem. Phys.* 153:044130
148. Piana S, Laio A. 2007. A bias-exchange approach to protein folding. *J. Phys. Chem. B* 111(17):4553–59
149. Plattner N, Doerr S, de Fabritiis G, Noé F. 2017. Complete protein-protein association kinetics in atomic detail revealed by molecular dynamics simulations and Markov modelling. *Nat. Chem.* 9:1005–11
150. Pohorille A, Jarzynski C, Chipot C. 2010. Good practices in free-energy calculations. *J. Phys. Chem. B* 114:10235–53
151. Ponder JW, Wu C, Ren P, Pande VS, Chodera JD, et al. 2010. Current status of the AMOEBA polarizable force field. *J. Phys. Chem. B* 114:2549–64
152. Postma JPM, Berendsen HJC, Haak JR. 1982. Thermodynamics of cavity formation in water: a molecular dynamics study. *Faraday Symp. Chem. Soc.* 17:55–67
153. Provasi D, Artacho MC, Negri A, Mobarec JC, Filizola M. 2011. Ligand-induced modulation of the free-energy landscape of G protein-coupled receptors explored by adaptive biasing techniques. *PLOS Comput. Biol.* 7:e1002193
154. Raniolo S, Limongelli V. 2020. Ligand binding free-energy calculations with funnel metadynamics. *Nat. Protoc.* 15(9):2837–66
155. Riahi S, Rowley CN. 2014. Why can hydrogen sulfide permeate cell membranes? *J. Am. Chem. Soc.* 136(43):15111–13
156. Rodinger T, Howell PL, Pomès R. 2005. Absolute free energy calculations by thermodynamic integration in four spatial dimensions. *J. Chem. Phys.* 123:34104
157. Rodinger T, Howell PL, Pomès R. 2008. Calculation of absolute protein-ligand binding free energy using distributed replica sampling. *J. Chem. Phys.* 129:155102
158. Roh SH, Shekar M, Singharoy M, Chipot C, Chiu W, Wilkens S. 2020. Cryo-EM and MD infer water-mediated proton transport and autoinhibition mechanisms of V_o complex. *Sci. Adv.* 6:eabb9605
159. Rosta E, Hummer G. 2015. Free energies from dynamic weighted histogram analysis using unbiased Markov state model. *J. Chem. Theory Comput.* 11(1):276–85
160. Roux B. 1995. The calculation of the potential of mean force using computer simulations. *Comput. Phys. Commun.* 91:275–82
161. Roux B, Nina M, Pomès R, Smith JC. 1996. Thermodynamic stability of water molecules in the Bacteriorhodopsin proton channel: a molecular dynamics and free energy perturbation study. *Biophys. J.* 71:670–81
162. Salomon-Ferrer R, Case DA, Walker RC. 2013. An overview of the Amber biomolecular simulation package. *WIREs Comput. Mol. Sci.* 3:198–210
163. Shaw D, Deneroff M, Dror R, Kuskin J, Larson R, et al. 2007. Anton, a special-purpose machine for molecular dynamics simulation. *ACM SIGARCH Comput. Archit. News* 35:1–12
164. Shirts MR, Chodera JD. 2008. Statistically optimal analysis of samples from multiple equilibrium states. *J. Chem. Phys.* 129:124105

165. Shirts MR, Mobley DL, Chodera JD. 2007. Alchemical free energy calculations: ready for prime time? In *Annual Reports in Computational Chemistry*, Vol. 3, ed. DC Spellmeyer, R Wheeler, pp. 41–59. Amsterdam: Elsevier
166. Singh N, Warshel A. 2010. Absolute binding free energy calculations: on the accuracy of computational scoring of protein-ligand interactions. *Proteins* 78(7):1705–23
167. Singharoy A, Chipot C, Moradi M, Schulten K. 2017. Chemomechanical coupling in hexameric protein-protein interfaces harnesses energy within V–type ATPases. *J. Am. Chem. Soc.* 139:293–310
168. Sugita Y, Kitao A, Okamoto Y. 2000. Multidimensional replica-exchange method for free-energy calculations. *J. Chem. Phys.* 113:6042–51
169. Suh D, Jo S, Jiang W, Chipot C, Roux B. 2019. String method for protein–protein binding free-energy calculation. *J. Chem. Theory Comput.* 15:5829–44
170. Suh D, Radak BK, Chipot C, Roux B. 2018. Enhanced configurational sampling with hybrid non-equilibrium molecular dynamics/Monte Carlo propagator. *J. Chem. Phys.* 148:014101
171. Swift RV, Amaro RE. 2013. Back to the future: Can physical models of passive membrane permeability help reduce drug candidate attrition and move us beyond QSPR? *Chem. Biol. Drug Des.* 81:61–71
172. Szabo A, Schulten K, Schulten Z. 1980. First passage time approach to diffusion controlled reactions. *J. Chem. Phys.* 72:4350–57
173. Takada N, Futatsugi N, Narumi AST, Okimoto N, Kawai HHA, et al. 2003. Parallelized simulation of molecular dynamics with a special-purpose computer: MDGRAPE–2. *Genome Inform.* 14:625–26
174. Tembe BL, McCammon JA. 1984. Ligand–receptor interactions. *Comput. Chem.* 8:281–83
175. Teo I, Mayne CG, Schulten K, Lelièvre T. 2016. Adaptive multilevel splitting method for molecular dynamics calculation of benzamidine-trypsin dissociation time. *J. Chem. Theory Comput.* 12(6):2983–89
176. Thompson AP, Aktulga HM, Berger R, Bolintineanu DS, Brown WM, et al. 2022. LAMMPS—a flexible simulation tool for particle-based materials modeling at the atomic, meso, and continuum scales. *Comput. Phys. Commun.* 271:108171
177. Tiwary P, Berne BJ. 2016. Spectral gap optimization of order parameters for sampling complex molecular systems. *PNAS* 113(11):2839–44
178. Torrie GM, Valleau JP. 1977. Monte Carlo study of phase separating liquid mixture by umbrella sampling. *J. Chem. Phys.* 66:1402–8
179. Tse C, Wickstrom L, Kvaratskhelia M, Gallicchio E, Levy R, Deng N. 2020. Exploring the free-energy landscape and thermodynamics of protein-protein association. *Biophys. J.* 119(6):1226–38
180. Tse CH, Comer J, Sang Chu SK, Wang Y, Chipot C. 2019. Affordable membrane permeability calculations: permeation of short-chain alcohols through pure-lipid bilayers and a mammalian cell membrane. *J. Chem. Theory Comput.* 15(5):2913–24
181. Tse CH, Comer J, Wang Y, Chipot C. 2018. Link between membrane composition and permeability to drugs. *J. Chem. Theory Comput.* 14(6):2895–909
182. Valleau JP, Card DN. 1972. Monte Carlo estimation of the free energy by multistage sampling. *J. Chem. Phys.* 57:5457–62
183. Valsson O, Parrinello M. 2014. Variational approach to enhanced sampling and free energy calculations. *Phys. Rev. Lett.* 113(9):090601
184. van Duijneveldt S, Frenkel D. 1992. Computer-simulation study of free-energy barriers in crystal nucleation. *J. Chem. Phys.* 96:4655–68
185. Velez-Vega C, Gilson MK. 2013. Overcoming dissipation in the calculation of standard binding free energies by ligand extraction. *J. Comput. Chem.* 34(27):2360–71
186. Votapka LW, Jagger BR, Heyneman AL, Amaro RE. 2017. SEEKR: simulation enabled estimation of kinetic rates, a computational tool to estimate molecular kinetics and its application to trypsin-benzamidine binding. *J. Phys. Chem. B* 121(15):3597–606
187. Wang F, Landau DP. 2001. An efficient, multiple range random walk algorithm to calculate the density of states. *Phys. Rev. Lett.* 86:2050–53
188. Wang J, Deng Y, Roux B. 2006. Absolute binding free energy calculations using molecular dynamics simulations with restraining potentials. *Biophys. J.* 91:2798–814
189. Wang Y, Harrison CB, Schulten K, McCammon JA. 2011. Implementation of accelerated molecular dynamics in NAMD. *Comput. Sci. Discov.* 4:015002

190. Wang Y, Ribeiro JML, Tiwary P. 2019. Past–future information bottleneck framework for sampling molecular reaction coordinate, thermodynamics and kinetics. *Nat. Commun.* 10:3573
191. Warshel A. 1984. Simulating the energetics and dynamics of enzymatic reactions. In *Specificity in Biological Interactions*, ed. C Chagas, B Pullman, pp. 59–81. Berlin: Springer
192. Wehmeyer C, Noé F. 2018. Time-lagged autoencoders: deep learning of slow collective variables for molecular kinetics. *J. Chem. Phys.* 148(24):241703
193. E W, Ren W, Vanden-Eijnden E. 2002. String method for the study of rare events. *Phys. Rev. B* 66:052301
194. E W, Ren W, Vanden-Eijnden E. 2005. Transition pathways in complex systems: reaction coordinates, isocommittor surfaces, and transition tubes. *Chem. Phys. Lett.* 413:242–47
195. E W, Vanden-Eijnden E. 2010. Transition-path theory and path-finding algorithms for the study of rare events. *Annu. Rev. Phys. Chem.* 61:391–420
196. Widom B. 1963. Some topics in the theory of fluids. *J. Chem. Phys.* 39:2808–12
197. Widom B. 1982. Potential distribution theory and the statistical mechanics of fluids. *J. Phys. Chem.* 86:869–72
198. Wojtas-Niziurski W, Meng Y, Roux B, Bernèche S. 2013. Self-learning adaptive umbrella sampling method for the determination of free energy landscapes in multiple dimensions. *J. Chem. Theory Comput.* 9:1885–95
199. Woo HJ, Roux B. 2005. Calculation of absolute protein–ligand binding free energy from computer simulations. *PNAS* 102:6825–30
200. Woods CJ, Essex JW, King MA. 2003. The development of replica-exchange-based free-energy methods. *J. Phys. Chem. B* 107:13703–10
201. Ytreberg FM, Zuckerman DM. 2006. Simple estimation of absolute free energies for biomolecules. *J. Chem. Phys.* 124:104105
202. Zavitsanou S, Tsengenes A, Papadourakis M, Amendola G, Chatzigoulas A, et al. 2021. FEPrepare: a web-based tool for automating the setup of relative binding free energy calculations. *J. Chem. Inf. Model.* 61(9):4131–38
203. Zhao T, Fu H, Lelièvre T, Shao X, Chipot C, Cai W. 2017. The extended generalized adaptive biasing force algorithm for multidimensional free-energy calculations. *J. Chem. Theory Comput.* 13:1566–76
204. Zheng L, Chen M, Yang W. 2008. Random walk in orthogonal space to achieve efficient free-energy simulation of complex systems. *PNAS* 105:20227–32
205. Zimmerman MI, Porter JR, Ward MD, Singh S, Vithani N, et al. 2021. SARS-CoV-2 simulations go exascale to predict dramatic spike opening and cryptic pockets across the proteome. *Nat. Chem.* 13(7):651–59
206. Zuckerman DM, Chong LT. 2017. Weighted ensemble simulation: review of methodology, applications, and software. *Annu. Rev. Biophys.* 46:43–57
207. Zuo Z, Wang B, Weng J, Wang W. 2015. Stepwise substrate translocation mechanism revealed by free energy calculations of doxorubicin in the multidrug transporter AcrB. *Sci. Rep.* 5:13905
208. Zwanzig RW. 1954. High-temperature equation of state by a perturbation method. I. Nonpolar gases. *J. Chem. Phys.* 22:1420–26